Supplemental Material for: Dynamics of a large population of red blood cells under shear flow

C. MINETTI[1], V. AUDEMAR[2], T. PODGORSKI[2] AND G. COUPIER[2]

[1] Service de chimie physique EP, Université libre de Bruxelles, 50, avenue Frankin-Roosevelt, CP16/62, B-1050 Brussels, Belgium. [2] Université Grenoble Alpes, CNRS, LIPhy, F-38000 Grenoble, France.

(Received 7 January 2019)

1. Cell orientation and Jeffery's orbits

For exhaustiveness and for the comfort of the reader, we give additional details for the section 2 of the paper. In particular, we present the other commonly used convention for Euler angles and the associated Jeffery equation.

We consider cells placed in a shear flow with flow direction Oz', shear gradient direction Oy' and vorticity axis Ox'. To characterize the orientation and motion of cells, we shall use the Euler angles. Let us consider, as a first approximation for a RBC, an ellipsoid of equation

$$r^2x^2 + y^2 + z^2 = 1. \tag{1.1}$$

r is the aspect ratio, which will be larger than 1 here (oblate ellipsoid). This ellipsoid may rotate and we use the Euler angles to describe this rotation in the fixed coordinate system $Ox'y'z'$ that coincides initially with the system $Oxyz$ associated with the ellipsoid.

When using Euler angles, one must take care to specify which convention is used to make the successive rotations, in particular if a rigid body is attached to the rotating system. We shall review the two conventions usually used in the RBC dynamics literature.

In the original paper by Jeffery (Jeffery (1922)), θ is obtained by rotation around the $Oz' = Oz$ axis, then ϕ is obtained by rotation around the Ox' axis, such that it is defined as the angle between the planes $Ox'y'$ and $Ox'x$ (see Fig. 1). A third angle denotes rotation around the Ox axis and will not be used here, as those rotations around the axis of symmetry of the cell will not be measured. In the absence of such a rotation, ϕ is also the angle between Oz and Oz'. With this convention, when $\phi = 0$ and $\theta = 90°$, the cell face is in the $Ox'z'$ plane.

If the cells are viewed from the vorticity axis Ox', the angle ϕ can be easily determined, as it is the angle between Oy' and the projection of the cell axis of revolution Ox onto the shear plane $Oy'z'$, which is the small axis of symmetry of the projection of the cell onto the shear plane.

If the cells are viewed from the velocity gradient axis Oy', as in our experiments, the angle Ψ defined as the angle between Ox' and the projection of the cell axis of revolution Ox onto the plane $Ox'z'$, can be easily determined (see. Fig. 1). This angle is also the angle made by the projection of the cell compared to the flow direction. Ψ is related to θ and ϕ through $\tan\Psi = \tan\theta \sin\phi$.

If the shear flow in the z' direction with y' the shear gradient direction and x' the vorticity direction, the motion of a rigid ellipsoid in creeping flow is given by (Jeffery (1922)):

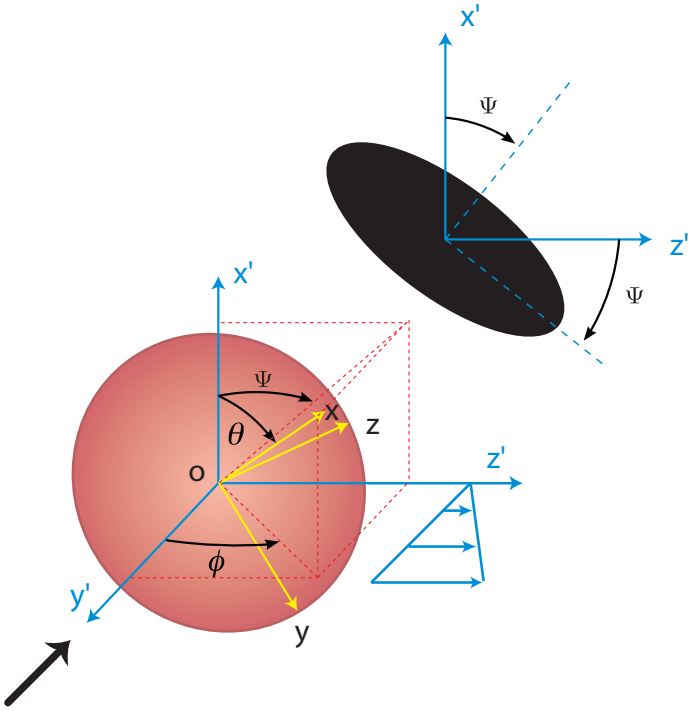

FIGURE 1. The Euler angles used to describe the flipping regime. Convention used in Jeffery (1922) and in the paper. The large black arrow shows the viewing direction in the experiments, where projection on the $x'z'$ plane is seen (black ellipse).

$$\tan\theta = \frac{\mathrm{C}}{r(r^{-2}\cos^2\phi + \sin^2\phi)^{1/2}}, \tag{1.2}$$

$$\tan\phi = r^{-1}\,\tan\frac{\dot{\gamma}t}{r + r^{-1}}, \tag{1.3}$$

$$\dot{\theta} = \dot{\gamma}\frac{r^2 - 1}{r^2 + 1}\sin\theta\cos\theta\sin\phi\cos\phi, \tag{1.4}$$

$$\dot{\phi} = \frac{\dot{\gamma}}{1 + r^{-2}}(r^{-2}\cos^2\phi + \sin^2\phi), \tag{1.5}$$

with $\mathrm{C} \equiv r\tan\theta_0$ the orbit parameter. θ oscillates between θ_0 and $\arctan C$ (spinning motion).

We shall refer to these possible motions as flipping motions. Among them, $\theta_0 = 0°$ corresponds to what is called rolling motion (θ always equal to 0), while $\theta_0 = 90°$ corresponds to tumbling (θ always equal to 90°). Note that when $r > 1$, $\dot{\phi}$ is minimal when $\phi = 0$, which corresponds to the cell aligned with the flow direction.

We now comment on the convention used in Hinch & Leal (1979), which is the most common one in the general literature: first ϕ is obtained by rotation around the $Ox = Ox'$ axis and then θ denotes rotation around the intersection between the Oyz and $Oy'z'$ planes, which is called the line of nodes, and coincides with Oy if there is no rotation around the Ox axis. See Fig. 2. With this convention, when $\phi = 0$ and $\theta = \pi/2$, the cell face is in the $Ox'y'$ plane. For Eq. 1.5 to be still valid (in particular, to have minimal

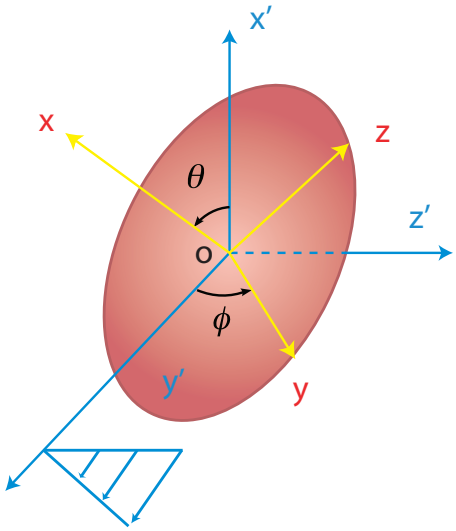

FIGURE 2. The Euler angles used in the standard convention, as in Hinch & Leal (1979) (See Fig. 1 in that paper).

velocity in this position) it imposes that the flow is in the Oy' direction, as in Hinch & Leal (1979). Note eventually that both schemes in Figs. 1 and 2 are the same providing the axis y' and z' are replaced by $-z'$ and y' on the right. If one wants to consider positive shear rates in both cases, as usually done by convention, it implies that the flow is reversed between the two cases, which eventually implies that a minus sign must be added in Eqs. 1.3 and 1.5 to be in agreement with the new scheme. This leads to the Eq. (3) in Hinch & Leal (1979).

2. Technical details for previous papers

We give here some technical details for the papers discussed in the article, in particular the notations used for the angles, and the description of regimes, that can differ between different papers.

2.1. *Experimental papers*

• Goldsmith & Marlow (1972): the outer viscosity η_0 is that of plasma, and the highest shear rate was 513 s^{-1}. High suspending fluid viscosity (520 mPa.s) and low shear rate (around 1 s^{-1}) is also considered. In the first experiment, the optical axis is in the vorticity direction Ox', which allows to directly determine ϕ (called ϕ_z in the original paper). On the other hand, determining θ (θ_z in the original paper) is not direct. If assumption on the cell shape is made, θ can be deduced from the aspect ratio of the projected shape onto the shear place $Oy'z'$. In the second experiment, which is similar to ours, the optical axis is the shear direction Oy'. They could measure Ψ, which is called ϕ_y in the original paper.

• Bitbol (1986): The cells are observed in a cone-plate geometry allowing for shear rates between 1 and 200 s^{-1}. Viscosity η_0 of the suspending medium was between 1 and 10 mPa.s. In this paper, ϕ and θ are defined as in the present work. The cells are observed

along the shear direction that is, rolling cell will appear edge-on. Because of the limited experimental time due to sedimentation, experiments in a large tube were carried on, in which no direct observation was possible. Instead, light scattering measurement were made, which allowed to make some assertions that remained qualitative by lack of theory for light scattering by RBCs.
Light scattering experiments allowed to measure the ratio between the number of cells in $C = 0$ orbits and the total number of cells aligned with the flow, as a function of η_0 and $\dot{\gamma}$. We make the following remark: at high shear rates, the cells aligned with the flow may be tank-treading cells, while at lower shear rates, tank-treading cells seen from the shear direction appears more or less circular, or even perpendicular to the flow, which makes the interpretation of Bitbol's result more complicate. In addition, non negligible contribution from cells in other flipping orbits may arise. Anyhow, for a given viscosity, this ratio first increases with the shear rate (apparition of orbits $C = 0$) then decreases (apparition of tank-treading cells).

• Dupire et al. (2012): The carrying fluid viscosities η_0 are 7 and 29 mPa.s, and the shear rate goes from 0 to 15 s^{-1} in the first case and to 2.7 s^{-1} in the second case. The cells flow in a large parallelepiped flow chamber where around 20 cells were followed individually thanks to two cameras that allow visualisation along both the shear and vorticity axis. Thanks to this, both angles Ψ and ϕ are measured. For Ψ, the discussion is centered on its maximal value (when the cell is seen edge-on), which is equal to the orbit angle θ_0. θ_0 and ϕ correspond respectively to $90 - \phi$ and θ in the original paper (see Fig.1 in Dupire et al. (2012)).

• Fischer & Korzeniewski (2013): They consider a Poiseuille flow (so probably only the increasing $\dot{\gamma}$ case is considered, though we do not know what the upstream conditions are) and observation along the vorticity axis direction Ox' are made. Their optical set-up allows the authors to detect cells that are edge-on so as to detect the flipping to tank-treading transition by counting the proportion of cells that are edge-on as a function of their radial position.

2.2. *Numerical simulations*

Numerous numerical studies are now devoted to the issue of RBC dynamics under shear flow. We focus here only on the most recent and relevant papers.

In Cordasco & Bagchi (2013), a state diagram with different shapes, in particular RBC shapes, is explored. This study is enriched in Cordasco et al. (2014) where they compare two different stress free shapes (for shear elasticity): biconcave discoid (as in Cordasco & Bagchi (2013)) and quasi spherical oblate ellipsoid. In Peng et al. (2014) , the effect of this stress free shape on the transition threshold to tank-treading is also discussed, while its influence on the orbital drift is discussed in Mendez & Abkarian (2018). In Sinha & Graham (2015), they consider the case of biconcave discoid as a stress free shape for shear elasticity but consider several cases of space-dependent spontaneous curvature that is, three cases of equilibrium shapes for bending energy : biconcave discoid, sphere and oblate ellipsoid. In all papers but in Peng et al. (2014) where a more complex modeling is introduced, the Skalak law for shear elasticity is chosen (it is justified in Sinha & Graham (2015) by comparison with other laws by simulating stretching with optical tweezers). η_0 is typically varied between 1 and 100 mPa.s and the stress $\eta_0\dot{\gamma}$ does not exceed 5 Pa (20 Pa in the more recent Mauer et al. (2018)).

The equivalence for notations for angles is:
• Cordasco & Bagchi (2013) : $\pi/2 - \theta_{xy}$ for θ and $\pi/2 - \phi$ for ϕ
• Cordasco et al. (2014) : $\pi/2 - \theta$ for θ and $\pi/2 - \phi$ for ϕ

- Peng et al. (2014) : $\pi/2 - \theta$ for θ and ψ for ϕ
- Sinha & Graham (2015) : ξ_0 for θ and $\pi/2 - \theta_0$ for ϕ
- Mendez & Abkarian (2018) : φ for θ and θ for ϕ

These papers establish a phase diagram that is qualitatively coherent with that partially drawn by experiments. It can be divided into four zones, the frontier of which depending on the considered equilibrium shapes (see Fig. 3 in the main paper). This diagram is obtained by starting with a cell with a given orientation θ, and following its time evolution. The diagram refers to the stationary dynamics to which it converges, at least when the simulation time is long enough. From the way the simulations are run, we can consider they correspond more to the increasing $\dot{\gamma}$ case (but to a sharp increase). None of the papers consider the decreasing case, nor the smoothly increasing case.

- (i) At small η_0, that is, in the physiological condition, the considered papers yield contradictory results. In Cordasco & Bagchi (2013), Cordasco et al. (2014) and Mendez & Abkarian (2018), it is found that flipping motions are not stable, and the cell exhibits drift (coupled with flipping) towards rolling. According to Cordasco & Bagchi (2013) and Cordasco et al. (2014), the time needed for this orbit to be reached does not depend on shear stress τ if the stress-free state is an oblate ellipsoid but decreases with increasing τ when the stress-free state is the discoid shape. The characteristic times are not given for low stress because of the shortness of the simulation run. For $\dot{\gamma} = 300$ s^{-1}, the characteristic time is less than 1 s. This is in agreement with Bitbol observation (see Bitbol 1986) of a typical time of order $100\times\dot{\gamma}^{-1}$. On the contrary, it is shown in Sinha & Graham (2015) that the stable configuration is tumbling for all explored shear stresses.
- (ii) In this high stress and high viscosity region, tank-treading is observed. If one starts with arbitrary θ, convergence towards tumbling is first observed, then tank-treading appears. As pointed out earlier, this tank-treading motion may be a rolling motion of a strongly deformed cell. Lack of information about the position of the material point originally located in the dimple does not allow to draw definitive conclusion.
- (ii') As τ decreases, more complex "tank-treading like" behavior appears : tank-treading with swinging (small oscillation of the cell around the vorticity axis), tank-treading with kayaking (small oscillations of the cell small axis across the shear plane that is, θ oscillates around 90°), hovering which is tank treading with the cell small axis off the shear plane. Note that those terms refer to the work by Cordasco *et al.*. In Sinha & Graham (2015), kayaking is referred as wobbling while hovering is denoted tilted tank-treading. The parameter ranges of all these states depend a lot on the equilibrium configuration of the cell and in all cases, they are rather narrow.
- (iii) In low stress and high viscosity region, Cordasco *et al.* found that orbits with low angle θ_0 are unstable and drift towards orbits with higher angles, which are stable. In two successive papers, they however found that orbits close to rolling drift towards rolling (see Cordasco & Bagchi 2013) or are unstable (see Cordasco et al. 2014). For spherical spontaneous curvature, Sinha and Graham observe Jeffery orbits (which they call kayaking) with angles that are close either to 0 or 90°. For oblate ellipsoidal spontaneous curvature they report some "flip-flopping motion" which they say to be close to tumbling without being a Jeffery orbit. However, they claim that this motion is identical to the "flipping motion" described in Dupire *et al.*, which is clearly described in this paper as a Jeffery orbit. Finally, in Mauer et al. (2018) and Mendez & Abkarian (2018), in the whole low stress region (until ~ 0.01 Pa, see Fig.2 in that paper), and whatever the viscosity, rolling is observed.

REFERENCES

Bitbol, M. 1986 Red blood cell orientation in orbit $c = 0$. Biophys. J. **49**, 1055.

Cordasco, D. & Bagchi, P. 2013 Orbital drift of capsules and red blood cells in shear flow. Phys. Fluids **25**, 091902.

Cordasco, D., Yazdani, A. & Bagchi, P. 2014 Comparison of erythrocyte dynamics in shear flow under different stress-free configurations. Phys. Fluids **26**, 041902.

Dupire, J., Socol, M. & Viallat, A. 2012 Full dynamics of a red blood cell in shear flow. Proc. Nat. Acad. Sci. USA **109**, 20808.

Fischer, T.M. & Korzeniewski, R. 2013 Threshold shear stress for the transition between tumbling and tank-treading of red blood cells in shear flow: dependence on the viscosity of the suspending medium. J. Fluid Mech. **736**, 351.

Goldsmith, H. L. & Marlow, J. 1972 Flow behaviour of erythrocytes. I. rotation and deformation in dilute suspensions. Proc. R. Soc. B **182**, 351.

Hinch, E. J. & Leal, L. G. 1979 Rotation of small non-axisymmetric particles in a simple shear flow. J. Fluid. Mech. **92**, 591–608.

Jeffery, G. B. 1922 The motion of ellipsoidal particles immersed in a viscous fluid. Proc. R. Soc. Lond. A **102**, 161.

Mauer, J., Mendez, S., Lanotte, L., Nicoud, F., Abkarian, M., Gompper, G. & Fedosov, D. A. 2018 Flow-induced transitions of red blood cell shapes under shear. Phys. Rev. Lett. **121**, 118103.

Mendez, S. & Abkarian, M. 2018 In-plane elasticity controls the full dynamics of red blood cells in shear flow. Phys. Rev. Fluids **3**, 101101.

Peng, Z., Mashayekh, A. & Zhu, Q. 2014 Erythrocyte responses in low-shear-rate flows: effects of non-biconcave stress-free state in the cytoskeleton. J. Fluid Mech. **742**, 96118.

Sinha, K. & Graham, M. D. 2015 Dynamics of a single red blood cell in simple shear flow. Phys. Rev. E **92**, 042710.